Physica Medica 81 (2021) 173–181

Contents lists available at ScienceDirect

Physica Medica

journal homepage: www.elsevier.com/locate/ejmp

Original paper

In vivo dosimetry in low-voltage IORT breast treatments with XR-RV3 radiochromic film

Sergio Lozares [a,*], Jose A. Font [a], Almudena Gandía [a], Arantxa Campos [b], Sonia Flamarique [b], Reyes Ibáñez [b], David Villa [a], Verónica Alba [a], Sara Jiménez [a], Mónica Hernández [a], Carmen Casamayor [c], Isabel Vicente [d], Ernesto Hernando [c], Patricia Rubio [d]

[a] Medical Physics Department. Miguel Servet University Hospital Zaragoza, Spain
[b] Radiation Oncology Department. Miguel Servet University Hospital Zaragoza, Spain
[c] Endocrine, Bariatric and Breast Surgery Unit. General and Digestive Surgery Department. Miguel Servet University Hospital Zaragoza, Spain
[d] Breast Unit. Gynaecology Department. Miguel Servet University Hospital Zaragoza, Spain

ARTICLE INFO

Keywords:
In vivo dosimetry
Radiochromic films
IORT
Electronic brachytherapy

ABSTRACT

Purpose: The objectives of the study were to establish a procedure for *in vivo* film-based dosimetry for intraoperative radiotherapy (IORT), evaluate the typical doses delivered to organs at risk, and verify the dose prescription.

Materials and methods: In vivo dose measurements were studied using XR-RV3 radiochromic films in 30 patients with breast cancer undergoing IORT using the Axxent® device (Xoft Inc.).

The stability of the radiochromic films in the energy ranges used was verified by taking measurements at different depths. The stability of the scanner response was tested, and 5 different calibration curves were constructed for different beam qualities. Six pieces of film were placed in each of the 30 patients. All the pieces were correctly sterilized and checked to ensure that the process did not affect the outcome. All calibration and dose measurements were analyzed using the Radiochromic.com software application.

Results: The doses were measured for 30 patients. The doses in contact with the applicator (prescription zone) were 19.8 ± 0.9 Gy. In the skin areas, the doses were as follows: 1–2 cm from the applicator, 1.86 ± 0.77 Gy; 2–5 cm, 0.73 ± 0.14 Gy; and greater than 5 cm, 0.28 ± 0.17 Gy. The dose delivered to the pectoral muscle (tungsten shielding disc) was 0.51 ± 0.27 Gy.

Conclusions: The study demonstrated the viability of XR-RV3 films for *in vivo* dose measurement in the dose and energy ranges applied in a complex procedure, such as breast IORT. The doses in organs at risk were far below the tolerances for cases such as those studied.

1. Introduction

Radiotherapy is an essential part of conservative treatment of breast cancer [1]. Given that 85% of recurrences in the breast occur adjacent to the primary tumor, there is growing interest in partial irradiation [2]. These techniques aim to reach effective doses of radiation in the tumor bed and to reduce the incidence of the adverse effects that result from irradiation of the whole breast. Partial irradiation techniques include intraoperative radiotherapy (IORT), which tries to improve local control of the disease by means of a single dose of ionizing radiation applied directly over the tumor bed during surgery [3].

IORT has been used as the only radiation modality in early stages in cases where the prognosis of breast cancer is favorable [4] and as a boost in the tumor bed of higher-risk patients [5], who will subsequently undergo external radiotherapy of the whole breast. These techniques include IORT with low-energy photons (50-kVp), which can be administered with various devices [6].

Evidence for IORT with low-energy photons in breast cancer is based on the "Targeted intraoperative radiotherapy versus whole breast radiotherapy for breast cancer (TARGIT-A trial)" study [7], which is an international, prospective, randomized, non-inferiority trial with more than 4000 patients. The trial demonstrated non-inferiority in terms of local recurrence rates with partial irradiation (50-kVp photons). For selected patients with early-stage breast cancer, a single dose of

* Corresponding autor at: Paseo Gran Vía 27, 50006 Zaragoza, Spain.
E-mail address: slozares@salud.aragon.es (S. Lozares).

https://doi.org/10.1016/j.ejmp.2020.12.011
Received 21 August 2020; Received in revised form 12 December 2020; Accepted 16 December 2020
Available online 16 January 2021

radiotherapy delivered during surgery using targeted IORT should be considered as an alternative to external beam radiotherapy delivered over several weeks.

Xoft Axxent® electronic brachytherapy™ (eBX) (Xoft, Inc., subsidiary of iCAD, San José, CA, USA) is a balloon-based high-dose-rate brachytherapy method that uses a disposable electronic radiation source, rather than a radioisotope, such as 192Ir. The radiation source is similar to that of the Intrabeam® device (Carl Zeiss Meditec, Inc., Oberkochen, Germany), which was used in the TARGIT trial [8].

The Axxent® S700 is a miniature X-ray device in a flexible catheter. The source is a vacuum tube (10 mm in length, 2 mm in diameter), encased in a cooling catheter (5.6 mm diameter). It is typically operated at 50 kVp with 300 μA of electrons striking a thin tungsten film target on the inner surface of a ceramic X-ray-transparent anode. It is used for conservative surgical treatment of breast cancer and irradiation of the tumor bed with a "balloon" applicator. A prescribed absorbed dose of 20 Gy is delivered to the target [9]. Furthermore, gynecological treatments for the endometrium [10] and cervix [11], as well as superficial skin treatments [12], may be administered with the same device.

One of the most important aspects of any radiotherapy approach is to ensure that the planned absorbed dose is equal to the absorbed dose administered to the patient. The many different methods for verifying radiotherapy include *in vivo* dosimetry during delivery of treatment [13,14]. The measurement of the dose absorbed in each procedure acts as a control of quality throughout the process.

Such an approach is essential in this type of IORT procedure, because the considerable dose gradient is compounded by tissue heterogeneity, which implies difficulty in estimating the skin dose with commercial treatment planning systems (TPSs) [15].

In addition to verifying the dose in the tumor bed, an *in vivo* dosimetry system enabled us to control the whole process, since the skin was appropriately protected and placement of protection of the pectoral muscle was adequate.

An excessively high absorbed dose delivered to the skin could lead to dermatitis or even necrosis [16,17].

This measurement procedure makes it possible to know the absorbed dose administered in cases where this type of problem occurs and to establish new protective measures for the future.

Previous studies estimated the doses in organs at risk for these patients based on preoperative computed tomography studies and calculations in the Eclipse v13.1 TPS (Varian Inc. Palo Alto, CA, USA) [18].

The objectives of the present study were to establish a procedure for *in vivo* film-based dosimetry for IORT, evaluate the typical dose delivered to organs at risk, and verify the prescribed dose delivered to the target.

Therefore, the energy response of the dosimeter used must be known and demonstrated to be accurate enough for purpose. The GafChromic™ XR-RV3 type, with an energy response range of 20 keV to 30 MeV and an absorbed dose range of 0.01 Gy to 30 Gy (according to the manufacturer) could be a good candidate that would fit the purpose of the measurement, although the process should be run carefully to avoid excessively high degrees of uncertainty [19]. The present study investigates the suitability of this radiochromic film model for this process and try to find out if the doses differ from those calculated by the TPS, especially for skin.

2. Materials and methods

The *in vivo* absorbed dose was measured in 30 patients with breast cancer who underwent surgery, during which they received IORT using the Axxent® device.

The absorbed dose prescribed to these patients was 20 Gy on the surface of the spherical balloon-type applicator in contact with the target (Fig. 1).

The volume of the "balloon" depends on the individual case; in the more than 500 patients treated, this ranged from 30 cm^3 to 90 cm^3, with 90% of cases between 30 cm^3 and 40 cm^3 (Table 1).

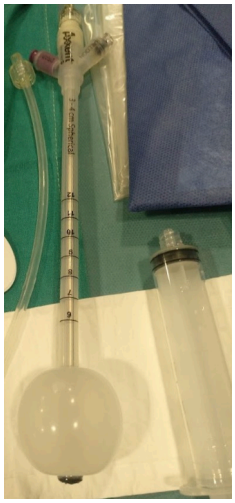

Fig. 1. Xoft's breast cancer IORT applicator (Type 3–4, vol.: 35 cm^3).

Radiochromic film was used as a detector. This approach is widely applied for verification of intensity-modulated radiotherapy treatments [20] and in *in vivo* dosimetry [21–23]. Various types of radiochromic film are commercially available [24], although the main difference between them is in the energy range and absorbed dose at which they show the optimal response.

These films can be cut into small pieces and then placed into a sterile envelope for use in the surgical field [23].

In the present study, *in vivo* absorbed doses were measured using XR-RV3 radiochromic film, which is specific for energies from upward of 20 kVp and absorbed doses of up to 30 Gy.

2.1. Film calibration

Appropriate calibration of the films is ensured by using a beam quality that is as close as possible to that used in the surgical procedure; calibrating to different energies can lead to marked differences in the reading of doses [25].

This method was used to estimate the doses at the various depths where the calibration curves were created in the measurement areas—in contact with the applicator (1 curve), in a series of skin areas (depending on the distance) (3 curves), and behind the shielding disk (1 curve)—up to a total of 5 different calibration curves.

Each of the calibration curves consists of 12 measurement steps. The 50-mm-diameter skin applicator was used in each step (beam quality equivalent to 1.56 mm Al according to the manufacturer). The calibration curve measured on the surface was used to calibrate the films in contact with the applicator. Subsequently, the remaining curves were

Table 1
Number of patients in the study by type of applicator and volume compared with the total number of patients treated up to May 2020.

Applicator			Total patients	Study Patients
Type	Volume (cm^3)	r (cm)	% (number)	% (number)
3–4	30	1.93	45.8 (232)	50 (15)
	35	2.03	32 (162)	33 (10)
	40	2.12	13.8 (70)	17 (5)
	45	2.21	5.5 (28)	
4–5	50	2.29	1.8 (9)	
	55	2.36	0	
	60	2.43	0.4 (2)	
	65	2.49	0.4 (2)	
5–6	65–130	2.49–3.14	0.2 (1)	
		Total	**506**	**30**

constructed at different depths for the measurements on skin and for the measurement behind the shielding disk. Radiochromic film should be calibrated with the same beam hardening as the verification to be carried out [26].

The reference dose was measured following the manufacturer's recommendations and using the TG-61 protocol with the ionization chamber calibrated for this energy. The ExRadin A20 ionization chamber (Standard Imaging Inc.), which was calibrated at the Accredited Dosimetry Calibration Laboratory of the University of Wisconsin-Madison (USA), was used as recommended (Table 2).

The in-air calibration method for low-energy X-ray beam was used, the reference depth for the determination of absorbed dose is at the phantom surface ($z_{ref} = 0$). The absorbed dose to water at the phantom surface shall be determined according to:

$$D_{w,z=0} = MN_K B_w P_{stem,air} \left[\left(\frac{\overline{\mu}_{en}}{\rho} \right)^{w}_{air} \right]_{air} \quad (1)$$

where M is the free-in-air chamber reading, with the center of the sensitive air cavity of the ionization chamber placed at the measurement point ($z_{ref} = 0$), corrected for temperature, pressure, ion recombination, polarity effect, and electrometer accuracy; N_K the air-kerma calibration factor; B_w the backscatter factor which accounts for the effect of the phantom scatter; $P_{stem,air}$ the chamber stem correction factor accounting for the change in photon scatter from the chamber stem between the calibration and measurement, and $\left[\left(\frac{\overline{\mu}_{en}}{\rho} \right)^{w}_{air} \right]_{air}$ the ratio for water-to-air of the mean mass energy-absorption coefficients averaged over the incident photon spectrum.

Devic et al. [25] reported a dependence on beam hardening in the response of radiochromic films, in measurements carried out with EBT3 radiochromic film and this same treatment equipment. The half-value layers (HVLs) of the Axxent® were estimated at different depths; at 2 cm, it was 1.468 mm Al. Since the radius of the average spherical ball applicator in the measurements carried out was 2.0 ± 0.1 cm, the use of the 50-mm applicator (HVL of 1.56 mm) could be suitable for creating the calibration curve used for the measurements on the surface of the "balloon".

The HVL given by the manufacturer for the 50-mm-diameter applicator used was verified by interposing 99.9% pure Al foils. The Axxent® operator manual suggests a source to detect a distance of 30 cm, with the filters placed 15 cm from the source for the HVL measurements of each applicator [27].

For all other depths, the corresponding HVL was calculated using the TM23342 PTW ionization chamber, which was calibrated in $N_{D,W}$ terms (Table 3) at the PTW Calibration Laboratory in Freiburg (Germany) for each configuration. The thickness that reduced the measurement to one half is obtained by interpolation.

Depth doses in water were obtained from dosemeasurements at the surface and by applying the TG-61 protocol. Percentage depth dose (PDD) data were provided by the factory based on measurements averaged over 10 sources with the 50-mm skin applicator used.

In addition, these results were verified by measuring with the TM23342 ionization chamber and plastic water slabs (PWDT: CIRS, Norfolk, VA), which were suitable for dosimetry of low-energy photon beams over the range of energies studied [28], based on the protocol for the TRS-398 [29]. The results obtained were similar.

Table 2
ExRadin A20 calibration data from the Accredited Dosimetry Calibration Laboratory of University of Wisconsin-Madison (USA).

Beam Quality ExRadin A20	Air Kerma Rate (mGy/s)	Air Kerma Calibration Coeff. (Gy/C)	Exposure Calibration Coeff. (R/C)	Calibration Uncertainty
UW60-M	1.79	3.884×10^8	4.434×10^{10}	1.0%
UW-50-M	2.02	3.927×10^8	4.483×10^{10}	1.0%

Table 3
TM23342 calibration data from the PTW Calibration Laboratory in Freiburg (Germany).

Beam Quality TM23342	$N_{D,W}$ (Gy/C)	Uncertainty
TW 70	1.102×10^9	3.3%
TW 50	1.087×10^9	3.3%

Three different areas could be distinguished for the absorbed dose administered to the skin depending on their distance from the surface of the "balloon": 1–2 cm, 2–5 cm, and >5 cm, as well as the area behind the disk that protects the chest wall during treatment of the left breast.

Using the skin applicator with a 50-mm surface diameter corresponding to an HVL of 1.56 mm in Al [30] (Fig. 2), and at several depths of solid water (0, 1.5, 3.5, 6 cm, and behind the shielding disk), 5 calibration curves were constructed; these were applied depending on the measurement area.

This configuration, although not exact, would aim to get closer to the clinical situation in order to obtain skin dose values that offer results closer to reality than those provided by the TPS calculation based algorithm.

Model XR-RV3 (batch 02141901) films were custom calibrated by cutting pieces of film measuring 5 × 5 cm^2. These were then appropriately marked and numbered to maintain their orientation in an Epson Expression 12,000 XL scanner.

As the film pieces must be sterilized for use in the surgical environment; sterilized film pieces were also used to construct the calibration curves in order to reduce uncertainty. The protocol of Méndez et al. [31] was followed. The films used for the calibration were scanned before and after irradiation; post-irradiation scanning was always performed 24 h later. The scanner was turned on 1 h before use, and 5 scans were made before scanning the films to warm up the light source, both before and after irradiation.

The films were scanned in RGB (48-bit) reflection mode with a

Fig. 2. Measurements with the Xoft 50 mm diameter skin applicator for calibration of XR-RV3 radiochromic films.

resolution of 75 dpi using Epson Scan software. The maximum range of optical density (OD) was applied, and all the image corrections and filters were switched off.

All films were scanned in portrait orientation, one by one, by placing the film in the center of the scanner. No correction was applied to address heterogeneity in the scanner response, since in no case was an area greater than 6 × 6 cm^2 in the central part of the scanner. Here, uniformity was 0.3%, following the method used by Richter et al. with the EBT1 films and the Epson V750 scanner [32]. Each film was scanned consecutively 5 times and saved as a TIFF file. The scanned films were subsequently read and calibrated using the multichannel method with the Multigaussian approach [33].

The pieces of film (5 × 5 cm^2) were exposed to absorbed doses of 0–25 Gy. The recommendation is to calibrate up to 20% above the maximum to be measured [34]; the maximum absorbed dose is the measurement in contact with the applicator, that is, 20 Gy.

The calibrations were made on 3 different days to verify the results, and 2 calibration curves (for each HVL) were constructed, namely, one from 0 to 25 Gy and the other from 0 to 5 Gy for the lowest absorbed doses in each of the configurations. The absorbed doses were lower on those areas of the skin at some distance from the applicator, thus enabling us to gain in accuracy.

Once the films were scanned, the files generated (both irradiated and non-irradiated films) were loaded into the Radiochromic.com v3.0 software application (Radiochromic SL, Benifaió, Spain).

The calibration curve with each of these images was calculated by selecting a region of interest (ROI) of 1 × 1 cm^2, to which the dose value that had previously been calculated using the ionization chamber was assigned. The software algorithm constructs the calibration curve that was used to measure the doses of the irradiated films used for the patients [33].

2.2. In vivo absorbed dose measurements

The same calibrated batch of films (XR-RV3, batch 02141901) is the one used to cut the pieces that are placed on/in patients with breast cancer who underwent surgery and were treated in situ with the Axxent® device.

The day before surgery, strips of film from the same batch were cut. Each strip was marked on the back with the numbers 0 to 6; the strips marked 1–6 were for use in the patient. The piece marked with a 0 was used to maintain the orientation. Each piece of film measured 1 × 1 cm^2.

The strips were cut and marked by a medical physicist wearing gloves in a darkened room using a special guillotine to ensure that the strips were uniform. These were stored in an opaque envelope, 2 to an envelope. The envelopes were then taken to the hospital sterilization service, where they were prepared for use in the operating room.

The strips of radiochromic film were sterilized in a gas plasma sterilizer (Sterrad 100S). This technology was designed to process thermosensitive materials that could withstand up to 55 °C and allow for sustained contact with the gas. The standard cycle time was approximately 54 min. Each cycle was monitored by the controls (physical, chemical, and biological). The material did not require aeration, as it did not leave toxic residues. Once the cycle was finished, the film was checked to ensure integrity and sealing of the packages and the process controls (physical, chemical, and biological) and was delivered to the Medical Physics Department.

Once the sterilized strips were returned to the Medical Physics Department, 1 envelope containing 2 strips was taken to each operation. One strip was left on the instrument table, where operating room staff cut the strips into small pieces measuring 1 × 1 cm^2 according to departmental guidelines and placed them on the patient's skin at different points (Fig. 3).

A piece was placed on the surface of the "balloon", at least 4 more were placed on the skin at different distances, and an additional piece was placed on the pectoral muscle behind the shielding disk, although only in patients whose left breast was being treated.

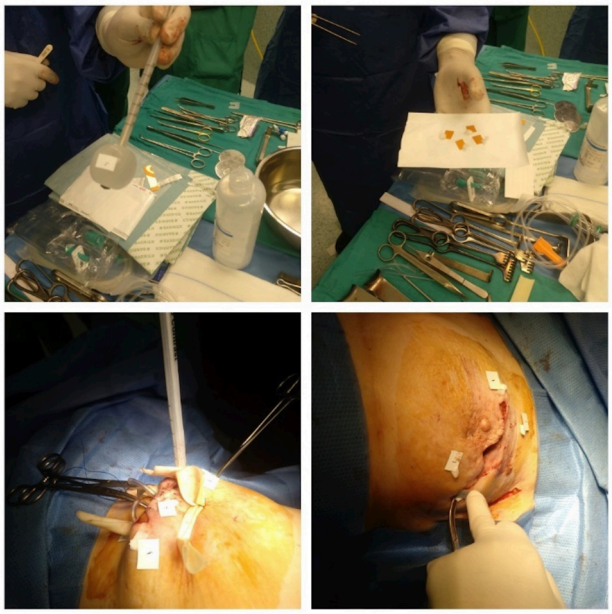

Fig. 3. Handling of radiochromic films in the sterile environment of the operating room. The strips are cut and placed on the patient and in contact with the applicator.

After placing the pieces of radiochromic film, the ultrasound image was acquired to ensure the position of the applicator and read the estimation of the distance between the applicator and the detectors. This step was repeated at the end of the procedure (Fig. 4).

After irradiation, the films were withdrawn by the surgeons and again placed in an opaque envelope, which was taken to the Medical Physics Department.

The pieces were left in an opaque envelope for 24 h until scanning under the same conditions as the films used for calibration.

The files generated after 5 scans of each piece were loaded into the Radiochromic.com environment, where they were read using previously generated calibration curves.

After this process, the pieces of film could be read in terms of dose.

Fig. 4. Measurement of the distance to the skin from the applicator with ultrasound image.

The file was then exported to ImageJ v1.52a (https://imagej.nih.gov/ij/), where a reading of the statistical parameters for the central area of each piece is obtained (0.5 × 0.5 cm^2).

The absorbed dose values thus obtained were represented as absorbed dose values very close to the applicator, absorbed doses in the skin depending on the distance to the applicator, and absorbed doses in the pectoral muscle.

In addition, the results for the skin were compared with the dose calculated by the Eclipse v13.1 TPS (Varian Inc., Palo Alto, CA, USA). The available algorithm was the TG-43 [35], with specific parameters for the Axxent® system but which does not correct for heterogeneity of the medium [36].

3. Results

3.1. Film calibration

The HVLs for the different depths were measured, and the results are shown in Table 4 for each chosen depth.

The results of *in vivo* dosimetry were grouped in ranges of distance to the source because of the difficulty in accurately measuring these distances to the order of millimeters. The mean distance of each range was chosen as the calibration depth except for distances greater than 5 cm, where calibration at a depth of 6 cm was used.

Agreement was good for the PDD curve measured with the TM23342 ionization chamber, the curve calculated from the data provided by the factory, and the measurement made with the ExRadin A20 chamber (Fig. 5).

Five different calibration curves were constructed to enhance the accuracy of results (Fig. 6). The netOD was calculated using Eq. (1) [37,38]:

$$netOD = OD_{exp} - OD_{unexp} = \log_{10}\frac{PV_{unexp} - PV_{bckg}}{PV_{exp} - PV_{bckg}} \quad (2)$$

where PV_{unexp} and PV_{exp} are the readings for unexposed and exposed areas of each film, respectively, and PV_{bckg} is the zero-light transmitted intensity value.

The multichannel method with the Multigaussian approach calibration algorithm uses the information from 3 reading channels—red, green, and blue—weighted differently based on the covariance matrix [33].

The Multigaussian method considers that, given a dose D, the probability of the response vector z (i.e., the vector with the responses z_k for each channel) obeys a multivariate Gaussian distribution

$$P(z|D) \tilde{} N_k(\mu(D), \Sigma(D)) \quad (3)$$

Here, k is the number of different channels (i.e., irradiated channels and optionally non-irradiated channels), μ is the vector of expected values of the response, and $\sum$ is the covariance matrix.

$$\Sigma_{ij} = cov[z_i, z_j] = E[(z_i - \mu_i)(z_j - \mu_j)] \quad (4)$$

Values were obtained for absorbed doses of 0–25 Gy in 12 steps. The measurements were then read and entered into the Radiochromic.com software application, which processes the results and calculates the calibration function.

Furthermore, once the energy response was resolved, 2 types of calibration curve were constructed: one for 0–25 Gy and the other for 0–5 Gy. The same results were obtained with both when calibrating the absorbed dose measured in the patients (Fig. 7).

Farah et al. [19] defined different scenarios for assessment of skin dose uncertainty with XR-RV3 Gafchromic™ films. In particular, Scenario B involved a well-defined laboratory calibration, whereas other

Table 4
Measured HVLs for the photon spectra at different distances from the Xoft 50-mm skin applicator in solid water.

Axxent® (Xoft) Energy: 50 kVp	
Depth in solid water from 50-mm skin applicator (cm)	HVL_{eq} (mm de Al)
0	1.56
1.5	1.9
3.5	2.3
6	2.8
Behind shielding disk	3.8

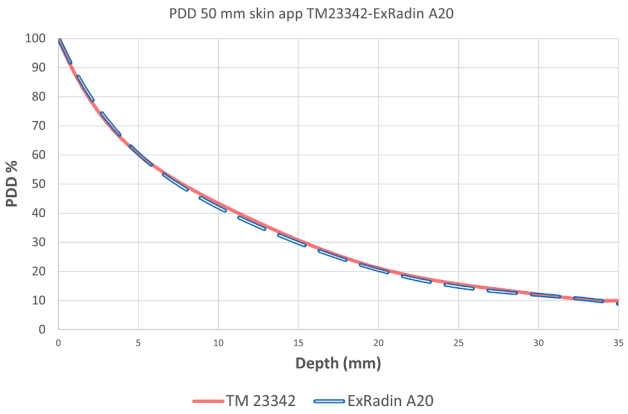

Fig 5. PDDs measured with the TM23342 ionization chamber and the curve calculated from the data provided by the factory and the measurement made with the ExRadin A20 chamber.

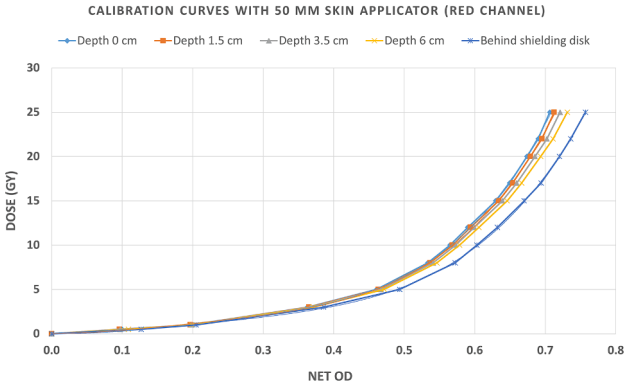

Fig. 6. Calibration curves in optical density versus dose (Gy) at the surface and at depths of 1.5, 3.5, 6 cm and "behind shielding disk" from the Xoft 50 mm diameter skin applicator.

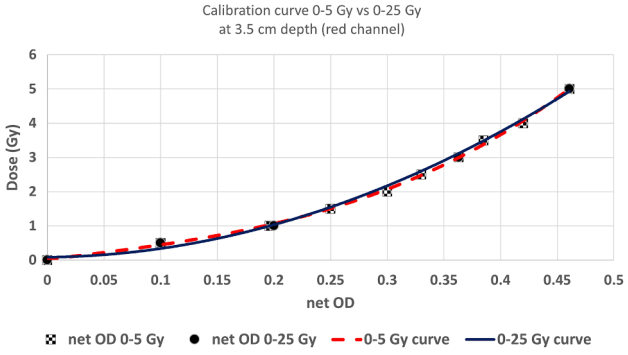

Fig. 7. Calibration curve of 0–5 Gy and 0–25 Gy (red channel) in optical density versus dose (Gy) for the 3.5 cm depth from applicator. (For interpretation of the references to colour in this figure legend, the reader is referred to the web version of this article.)

influencing parameters related to clinical application of dosimetry films are less controlled; such would be the scenario closest for the dose measurements in this study.

The values provided for PDD calculations with the TG-61 device had an uncertainty of 1% depending on the manufacturer. Verification of the PDD by measuring with another ionization chamber (Fig. 7) confirmed these results.

The uncertainty for this calculation step to other depths is assumed to be 3% following the recommendations of Ma et al. of the TG-61 [39].

The values of the uncertainties are shown in Table 5. The uncertainties are expressed as a percentage with a confidence interval of 68% (k = 1). The final expanded uncertainty has a 95% confidence interval (k = 2) [40].

The uncertainties for the calculation of the dose with ionization chamber are shown in the first part of the table.

The uncertainty in the value of the raw scan pixels, 0.8% (k = 1), is based on the standard deviation of the ROI measured on the darkest film, 25 Gy [41]. The uncertainty of the field flatness was calculated to be 0.3% (k = 1).

The uncertainties in the variability of the film-to-film response within a batch and the dose rate response were 1% and 1.5%, respectively. Note that the batch-to-batch variation in XR-RV3 film reported by Farah et al. [19] might be as high as 7% depending on the scenario; consequently, each new batch must be calibrated separately.

In the study, only 1 batch of film was used, and the low uncertainty in the response among the films could increase depending on the batch; a more representative value would be 2.5%, as reported by McCabe et al. [41].

The maximum difference between 2 of 5 successive scans was 0.3%.

Table 5
Uncertainty analysis for measured film data expressed as a percentage.

Determination of dose at other points in water		Uncertainty (%)	
N_K from calibration laboratory		1.0	Calibration Certificate
Effect of beam-quality difference between calibration and measurement		2.0	TG-61 [39]
Backscatter factor B_w		1.5	TG-61
$P_{stem,air}$		1.0	TG-61
$\left[\left(\frac{\overline{\mu}_{en}}{\rho}\right)^{w}_{air}\right]_{air}$		1.5	TG-61
In-air measurement in the user's beam		1.5	TG-61
Combined standard uncertainty for $D_{w,z=0}$		**3.6**	
Determination of dose at other points in water		3.0	TG-61
Combined standard uncertainty for $D_{w,z}$		**4.7**	
Uncertainty parameter	**Type A**	**Type B**	
Determination of dose at other points in water		4.7	
Beam uniformity		0.3	McCabe et al [41]
Film-to-film uniformity in 1 batch		1.0	Results Section D.
Dose-rate film response		1.5	McCabe et al [41]
Setup error and film positioning		0.3	McCabe et al [41]
Multichannel algorithm uncertainty		1.0	Vera-Sánchez et al[43]
Shutter error		0.1	McCabe et al [41]
Pixel value uncertainty within ROI	0.8		
Scan-to-scan uncertainty	0.1		
Sterilization process	0.5		
Scanner drift	0.1		
Quadratic sum	1.0	5.1	
A and B quadratic sum	5.2		
Dose per film response % uncertainty (k = 1)	5.2		
Dose per film response expanded % uncertainty (k = 2)	±10.4		

Assuming a rectangular distribution, this leads to a scan-to-scan uncertainty of 0.1% (k = 1). As this uncertainty value is less than the variation of the pixel value within the ROI, it was concluded that the light from the scanner did not cause the XR-RV3 film to darken measurably with each subsequent scan, in contrast with other types of radiochromic film [42].

The scanner drift was calculated by comparing the initial and final background scans while scanning the calibration films.

The uncertainty of the multichannel algorithm was studied using different scanner models. Vera-Sánchez et al. [43] reported uncertainty of 1% with the Epson 12000XL for low doses.

Any uncertainties in the orientation of the films or variations in humidity and temperature during transport and storage were reported owing to the special precautions in which the study was conducted. However, such eventualities should be considered if precautions are not optimal.

The final calibration curve traceable to the NIST extended the uncertainty for calculating the dose of the film (10.4% k = 2).

3.2. *In vivo* absorbed dose measurements

Dose measurements were performed with radiochromic films in 30 patients who underwent IORT with the Axxent® device based on the TARGIT study. A total of 166 measurements were recorded and grouped depending on their distance from the applicator (Table 6).

The dose values obtained for the target and the skin were compared with those given by the TPS at these distances. The values obtained for the *in vivo* dose are lower than those calculated by the TPS for all skin cases. Results for the prescription site (20 Gy vs 19.8 ± 0.9 Gy) revealed a less than 1% difference and are, therefore, not shown in the figure (Fig. 8).

4. Discussion

Beam hardening in IORT has been previously studied for the energies used here [44] based on the energy response of several models of radiochromic films [45], specifically XR-RV3 [41]. The various studies conducted to investigate the energy dependence of EBT GafChromic™ dosimetry films agree that different EBT film models were near tissue-equivalent [46] and that the responses of the films are energy-independent down to about 100 keV [47]. However, they varied in their findings in the energy range ≤100 keV [48]. In the photon energy range of 100–18 MeV, the absorbed-dose energy dependence is found to be energy-independent within 0.6%. However, below 100 keV, the absorbed-dose energy dependence of EBT varies by approximately 10% [46].

Given the beam hardening at different depths on the range of measurements in patients [25], measurements with different calibration curves have proven to be essential for validating *in vivo* absorbed dose readings and validating the results at the different sites studied [26].

In Devic et al. [25], values for HVL were used to select the appropriate calibration curve at each measurement point within the water phantom in the measurement range 2–6 cm. HVL values vary from 1.468 mm Al to 2.403 mm Al. The authors reported that in this region, the same signal could produce a relative dose measurement error of 5% if the beam hardening effect is ignored. They also remarked that accurate dose measurement using radiochromic films in low photon energies require the radiochromic film dosimetry system to be calibrated at beam qualities corresponding to measurement points, as a significant beam hardening effect occurs as a function of depth in water for the 50-kVp source. The radiation source and the 50-mm skin applicator together have an HVL of 1.56 mm according to the manufacturer; this was corroborated by experimental measurements. In the results reported by Devic et al., the source at the 2-cm depth has an HVL of 1.468 mm, which is very close to the abovementioned configuration. Thus, the curve for the measurement of the *in vivo* dose in contact with the "balloon" was calibrated to represent the prescription area (the average

Table 6
Results of *in vivo* dosimetry measurements grouped by organ (skin and pectoral muscle) and by distance from the applicator (tumor bed) in the case of skin.

Site of measurement	Average dose (Gy)	Dose range (Gy)	SD (Gy)	TPS Average dose (Gy)	"Balloon" volume (30/35/40) cm^3	No. of measurements
"Balloon" surface	19.8	18.8–20.7	0.9	20.0	(15/10/5)	30
1–2 cm from "balloon"	1.86	0.9–3.8	0.77	2.1	(35/20/5)	60
2–5 cm from "balloon"	0.73	0.4–0.9	0.14	1.0	(20/15/5)	40
>5 cm from "balloon"	0.28	0.03–0.4	0.17	0.4	(10/5/5)	20
Pectoral muscle	0.51	0.3–0.9	0.27		(9/5/2)	16

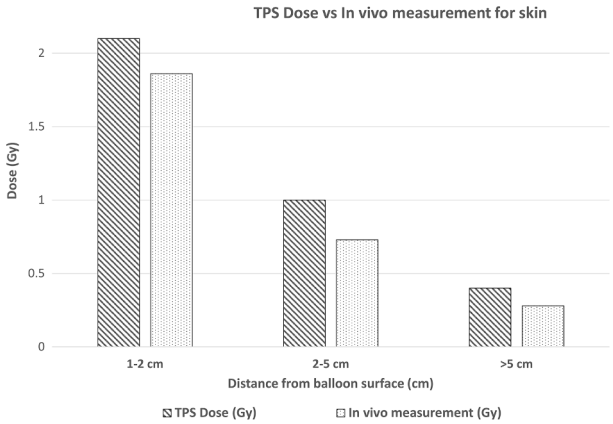

Fig 8. Dose values obtained for the target and the skin compared with those given by the TPS at these distances.

radius of the spherical "balloon" in the patients measured is 2.0 ± 0.1 cm). From there, curves were plotted for the depths of 1.5, 3.5, and 6 cm of solid water, representing depths of 3.5, 5.5, and 8 cm in the clinical environment. HVL values were obtained in accordance with those of Devic et al. [25].

The films were calibrated to reproduce the clinical conditions of beam hardening. The configurations chosen for each of the selected areas did not exactly reproduce the conditions of the beam in each situation. It would be impossible to have a calibration for each of the measurements, since, in addition, the distance of the pieces of film to the source placed on the patient, could not be measured with the same precision as the depth in water of the measurement in phantom.

The configurations outlined above were chosen to improve the results of the *in vivo* dose measurements.

The objective of *in vivo* measurements was to know if the dose calculated by the TPS in the different areas (clinically noteworthy) are reliable. According to the TG 186 report, for treatments with low energy in areas of breast tissue and near the surface (atomic number gradient border) the TG 43 overweighs the dose values, as shown by the present results. Farah et al. [19] reported that XR-RV3 films showed large variations (up to 15%) in radiation quality in both standard laboratory and clinical conditions and considered it mandatory to choose the appropriate calibration beam quality depending on the characteristics of the X-ray systems to be used in clinical practice. The energy dependence of radiochromic films lies mainly in their chemical composition, which changes from batch to batch [19]. Therefore, the film response must be checked for each batch. In this work, all the measurements were made with the same batch, with the result that uncertainty was reduced. Each of the films irradiated was calibrated with its corresponding calibration curve adjusted for beam hardening, with a gain in the accuracy of the results. Measurements at more distant areas of the skin were taken with a calibration curve of 0–5 Gy to increase accuracy owing to the low doses expected in this area.

The films used for calibration were previously sterilized, as were those used for *in vivo* measurement, so that uncertainty was reduced. Although the values of the sterilized and non-sterilized film were close for 0 Gy, in the case of 3.5 Gy, they were 1.6% for the red channel and 1.8% for the green channel.

The multichannel algorithm was used [33], thus optimizing each of the channels in the corresponding dose range. The algorithm gives more weight to the red channel in the initial intervals and to the green channel from 10 Gy onwards.

In the case of the Epson 12000XL scanner, the multichannel algorithms generated less uncertainty in the estimations for doses lower than 4 Gy [43] than for those obtained for skin measurements.

In clinical practice, the absorbed dose prescribed was 20 Gy on the surface of the "balloon" at the measurement points. Therefore, absorbed doses of around 20 Gy on the surface of the "balloon" and lower absorbed doses of around 0–5 Gy at the different points on the skin and behind the pectoral muscle were expected.

In addition to using the multichannel algorithm, 2 different sensitometric curves were plotted to obtain greater accuracy in each of the readings in such a way that there was a calibration of 0–5 Gy for the measurements expected for lower doses and another for the measurements expected for higher doses that cover up to 25 Gy.

The results showed that the absorbed dose ranges were clearly divided into low-dose and high-dose ranges, although when the readings of the film were taken with the expected doses below 5 Gy and a sensitometric curve of 0–25 Gy, the results differed by less than 2%.

Based on the TARGIT study, XR-RV3 radiochromic films were characterized by an energy response, dynamic dose range, and temperature independence that make them appropriate for *in vivo* dosimetry in IORT delivered to the breast.

Integration of the *in vivo* dose measurement procedure in the operating room was fast and did not interfere with any of the clinical stages. The surgeons quickly learned to manage the films, which arrived in opaque envelopes as numbered strips. The presence of the films in the surgical bed does not deform breast tissue or modify the dose absorbed around the tumor.

The absorbed dose values in the area of the tumor were as expected; the film was in direct contact with the "balloon".

The absorbed dose in the skin depends on the closeness to the radiation source. A minimum distance of 1 cm to any point on the skin was always maintained; this distance is measured and verified using ultrasound in the operating room by the surgeons.

Other detectors, such as thermoluminescence dosimeters (TLDs), have been used to measure doses in the skin. Fogg et al. [49] placed the TLDs at 8 points ranging from 5 to 15 mm from the incision in 57 patients and reported delivering the maximum dose in all 8 TLDs. The mean (SD) dose in the 57 patients was 2.93 (1.46) Gy. Avanzo et al. [23] placed the films in such a way that the closest were 1–2 cm from the applicator. The highest absorbed dose was 4.7 Gy, with a mean of 2.22 Gy in the closest area, which was similar to the average absorbed dose in the skin obtained in the study by Fogg et al.

Similarly, Ciocca et al. [14] found a mean deviation of 1.8% ± 4.7% between the expected dose and *in vivo* measurement with radiochromic films.

Other radiochromic film models have been used in IORT procedures [22,50].

Petoukhova et al. [22] measured the *in vivo* dose for electron IORT with MOSFET dosimetry for 27 patients and Gafchromic™ film dosimetry for 20 patients. The entry dose for the breast tissue, as measured with MOSFETs (mean value 22.3 Gy, SD 3.4%), agreed with the

expected dose (mean value 21.9 Gy) to within 1.7%. The dose in breast tissue, as measured with radiochromic films (mean value 23.50 Gy), was on average within 0.7% (SD = 3.7%, range –5.5% to 5.6%) of the prescribed dose of 23.33 Gy.

Also in electron IORT, Avanzo et al. [50] reported that the *in vivo* dose was 3.1% larger (one-sample *t* test, $p \ll 0.001$) than the prescribed dose, with a standard deviation of 4.7% and 95% confidence intervals of –6.4% and 12.4% measured using MOSFET detectors.

The absorbed doses measured in the skin of the study patients were lower on average (1.93 Gy), although very close to those of Avanzo et al. [23]. The maximum absorbed dose was 3.8 Gy, which was always below the threshold of 6 Gy, the limit for skin damage after a single exposure to X-rays [51]. Dose measurements in the skin at greater distances from the applicator revealed a rapid decrease, to a few cGy at >5 cm from the applicator, as was expected.

Therefore, this procedure, which combines surgery with radiotherapy, involves no significant problems in terms of risk of cutaneous adverse effects, providing that some distance is maintained between the borders and the applicator during irradiation (at least 1 cm according to the protocol).

Measurements in the pectoral muscle (shielded by tungsten), which were taken in the left breast, reveal that doses are sufficiently low not to expect damage to the heart as administered during the procedure.

The doses measured for the skin were markedly lower than those obtained in the TPS.

For low-energy sources, the photoelectric process is dominant; differences in mass-energy absorption coefficients between various tissues and water [52] could result in significant dose differences depending on the medium chosen for radiation transport and energy deposition.

Taylor demonstrated differences of up to 25% between dose to local medium and dose to water for breast tissue for the Xoft electronic miniature X-ray source with the dose ratio changing by nearly 25% over 5 cm [53].

The TG-43 parameters of a brachytherapy source were obtained in a homogeneous water phantom; however, in clinical practice, the brachytherapy sources are located inside the patient's tissues. The different mass absorption coefficients, radiation scattering, and attenuations in materials with different compositions would alter the dose distribution in comparison with water. There are also other tissues inside the human body with more differences in density, atomic number, and chemical compositions (e.g. bone, breast, lung), for which many more discrepancies are observed in TG-43 parameters than in the water phantom [54].

Duque et al. [55] reported the dosimetric impact of replacing the TG-43 algorithm with a model-based dose calculation for liver brachytherapy and found that the dose calculated with TG-186 was on average lower than that calculated with TG-43.

White et al. [56] compared TG-43 and TG-186 in breast irradiation using Axxent® and reported that all simulated heterogeneous models yielded a dose that was smaller than the dose-volume-histogram metrics, which was dependent on the method of dose reporting and patient geometry. Based on a prescribed dose of 34 Gy, the average D90 to PTV was reduced by between ~4% and ~40%, depending on the scoring method, compared with the TG-43 result. The peak skin dose was also reduced by 10%-15% owing to the absence of backscatter not accounted for in TG-43. Therefore, the results obtained on skin were expected to be lower than those obtained with the TPS.

The discrepancies between the *in vivo* dosimetry measurement results and those given by the TPS were larger than expected according to the estimated uncertainty which is explained considering the heterogeneous media influence in the case of low energies.

5. Conclusions

This study demonstrates the viability of *in vivo* dosimetry using radiochromic film and the appropriateness of the XR-RV3 model for IORT, in terms of dosing range and energy response. Although one should be careful in the film calibration procedure because the uncertainty was high and might be higher depending on the calibration scenario.

The radiotherapy procedure used is difficult to verify in any other way. The approach used in the present study guarantees the quality of treatment, since the dose was verified directly.

The model used shows that the features and versatility of the radiochromic film model studied are suitable for this procedure, since the film is specifically designed for the dose and energy ranges applied.

In addition, the doses delivered to the surgical bed were confirmed to be appropriate and those delivered to the organs at risk were sufficiently low the results measured on skin were lower than those calculated by the TPS.

The results for and the simple implementation of the procedure in the operating room suggest that this approach should continue to be used owing to the associated increase in quality.

Declaration of Competing Interest

The authors declare that they have no known competing financial interests or personal relationships that could have appeared to influence the work reported in this paper.

References

[1] Veronesi U, Salvadori B, Luini A, Banfi A, Zucali R, Del Vecchio M, et al. Conservative treatment of early breast cancer. Long-term results of 1232 cases treated with quadrantectomy, axillary dissection, and radiotherapy. Ann Surg 1990;211:250–9.

[2] Effect of radiotherapy after breast-conserving surgery on 10-year recurrence and 15-year breast cancer death: meta-analysis of individual patient data for 10 801 women in 17 randomised trials. Lancet 2011;378:1707–16. https://doi.org/10.1016/S0140-6736(11)61629-2.

[3] Reitsamer R, Sedlmayer F, Kopp M, Kametriser G, Menzel C, Glueck S, et al. Concepts and techniques of intraoperative radiotherapy (IORT) for breast cancer. Breast Cancer 2008;15:40–6. https://doi.org/10.1007/s12282-007-0001-4.

[4] Cuncins-Hearn A, Saunders C, Walsh D, Borg M, Buckingham J, Frizelle F, et al. A systematic review of intraoperative radiotherapy in early breast cancer. Breast Cancer Res Treat 2004;85:271–80. https://doi.org/10.1023/B:BREA.0000025411.77758.1e.

[5] Sedlmayer F, Reitsamer R, Wenz F, Sperk E, Fussl C, Kaiser J, et al. Intraoperative radiotherapy (IORT) as boost in breast cancer. Radiat Oncol 2017;12. https://doi.org/10.1186/s13014-016-0749-9.

[6] Eaton DJ. Electronic brachytherapy–current status and future directions. Br J Radiol 2015;88:20150002. https://doi.org/10.1259/bjr.20150002.

[7] Vaidya JS, Joseph DJ, Tobias JS, Bulsara M, Wenz F, Saunders C, et al. Targeted intraoperative radiotherapy versus whole breast radiotherapy for breast cancer (TARGIT-A trial): an international, prospective, randomised, non-inferiority phase 3 trial. Lancet 2010;376:91–102. https://doi.org/10.1016/S0140-6736(10)60837-9.

[8] Dickler A, Dowlatshahi K. Xoft Axxent electronic brachytherapy™. Expert Rev Med Devices 2009;6:27–31. https://doi.org/10.1586/17434440.6.1.27.

[9] Dickler A, Ivanov O, Francescatti D. Intraoperative radiation therapy in the treatment of early-stage breast cancer utilizing xoft axxent electronic brachytherapy. World J Surg Oncol 2009;7:24. https://doi.org/10.1186/1477-7819-7-24.

[10] Lozares-Cordero S, Font-Gómez JA, Gandía-Martínez A, Méndez-Villamón A, Villa-Gazulla D, Miranda-Burgos A, et al. Postoperative endometrial cancer treatments with electronic brachytherapy source. J Radiother Pract 2019;18:16–20. https://doi.org/10.1017/S1460396918000353.

[11] Lozares-Cordero S, Font-Gómez JA, Gandía-Martínez A, Miranda-Burgos A, Méndez-Villamón A, Villa-Gazulla D, et al. Treatment of cervical cancer with electronic brachytherapy. J Appl Clin Med Phys 2019;20:78–86. https://doi.org/10.1002/acm2.2019.20.issue-710.1002/acm2.12657.

[12] Safigholi H, Song WY, Meigooni AS. Optimum radiation source for radiation therapy of skin cancer. J Appl Clin Med Phys 2015;16:219–27. https://doi.org/10.1120/jacmp.v16i5.5407.

[13] Essers M, Mijnheer B. In vivo dosimetry during external photon beam radiotherapy. Int J Radiat Oncol 1999;43:245–59. https://doi.org/https://doi.org/10.1016/S0360-3016(98)00341-1.

[14] Ciocca M, Orecchia R, Garibaldi C, Rondi E, Luini A, Gatti G, et al. In vivo dosimetry using radiochromic films during intraoperative electron beam radiation therapy in early-stage breast cancer. Radiother Oncol 2003;69:285–9. https://doi.org/10.1016/j.radonc.2003.09.001.

[15] Beaulieu L, Carlsson Tedgren Å, Carrier J-F, Davis SD, Mourtada F, Rivard MJ, et al. Report of the Task Group 186 on model-based dose calculation methods in brachytherapy beyond the TG-43 formalism: current status and recommendations

for clinical implementation. Med Phys 2012;39:6208–36. https://doi.org/10.1118/1.4747264.
[16] Chua BH, Henderson MA, Milner AD. Intraoperative radiotherapy in women with early breast cancer treated by breast-conserving therapy. ANZ J Surg 2011;81:65–9. https://doi.org/10.1111/j.1445-2197.2010.05431.x.
[17] Joseph DJ, Bydder S, Jackson LR, Corica T, Hastrich DJ, Oliver DJ, et al. Prospective trial of intraoperative radiation treatment for breast cancer. ANZ J Surg 2004;74:1043–8. https://doi.org/10.1111/j.1445-1433.2004.03264.x.
[18] Gandía A, Lozares S, Font-Gómez JA, Molina G, Ibañez R, García-Mur MC, et al. EP-1314: breast treatments with Axxent equipment. Comparison with Mammosite for skin, lung and heart dose. Radiother Oncol 2018;127:S721. https://doi.org/10.1016/S0167-8140(18)31624-4.
[19] Farah J, Trianni A, Ciraj-Bjelac O, Clairand I, De Angelis C, Delle Canne S, et al. Characterization of XR-RV3 GafChromic® films in standard laboratory and in clinical conditions and means to evaluate uncertainties and reduce errors. Med Phys 2015;42:4211–26. https://doi.org/10.1118/1.4922132.
[20] Zeidan OA, Stephenson SAL, Meeks SL, Wagner TH, Willoughby TR, Kupelian PA, et al. Characterization and use of EBT radiochromic film for IMRT dose verification. Med Phys 2006;33:4064–72. https://doi.org/10.1118/1.2360012.
[21] Severgnini M, de Denaro M, Bortul M, Vidali C, Beorchia A. In vivo dosimetry and shielding disk alignment verification by EBT3 GAFCHROMIC film in breast IOERT treatment. J Appl Clin Med Phys 2015;16:112–20. https://doi.org/10.1120/jacmp.v16i1.5065.
[22] Petoukhova A, Rüssel I, Nijst-Brouwers J, van Wingerden Ko, van Egmond J, Jacobs D, et al. In vivo dosimetry with MOSFETs and GAFCHROMIC films during electron IORT for Accelerated Partial Breast Irradiation. Phys Medica 2017;44:26–33. https://doi.org/10.1016/j.ejmp.2017.11.004.
[23] Avanzo M, Rink A, Dassie A, Massarut S, Roncadin M, Borsatti E, et al. In vivo dosimetry with radiochromic films in low-voltage intraoperative radiotherapy of the breast. Med Phys 2012;39:2359–68. https://doi.org/10.1118/1.3700175.
[24] Devic S, Tomic N, Lewis D. Reference radiochromic film dosimetry: review of technical aspects. Phys Medica 2016;32:541–56. https://doi.org/https://doi.org/10.1016/j.ejmp.2016.02.008.
[25] Devic S, Liang LH, Tomic N, Bekerat H, Morcos M, Popovic M, et al. Dose measurements nearby low energy electronic brachytherapy sources using radiochromic film. Phys Med 2019;64:40–4. https://doi.org/10.1016/j.ejmp.2019.05.017.
[26] Devic S, Aldelaijan S, Bekerat H. Impact of inertia on possible fundamental drawbacks in radiochromic film dosimetry. Phys Med 2019;66:133–4. https://doi.org/10.1016/j.ejmp.2019.08.019.
[27] Xoft Inc. Axxent Electronic Brachytherapy System Operator Manual. Appendix J. 2009.
[28] Hill R, Kuncic Z, Baldock C. The water equivalence of solid phantoms for low energy photon beams. Med Phys 2010;37:4355–63. https://doi.org/10.1118/1.3462558.
[29] IAEA TRS 398. Absorbed Dose Determination in External Beam Radiotherapy. At Energy 2000. https://doi.org/10.1097/00004032-200111000-00017.
[30] Rong Y, Welsh JS. Surface applicator calibration and commissioning of an electronic brachytherapy system for nonmelanoma skin cancer treatment. Med Phys 2010;37:5509–17. https://doi.org/10.1118/1.3489379.
[31] Méndez I, Peterlin P, Hudej R, Strojnik A, Casar B. On multichannel film dosimetry with channel-independent perturbations. Med Phys 2014;41:1–10. https://doi.org/10.1118/1.4845095.
[32] Richter C, Pawelke J, Karsch L, Woithe J. Energy dependence of EBT-1 radiochromic film response for photon and electron beams readout by a flatbed scanner. Med Phys 2009;36:5506–14. https://doi.org/10.1118/1.3253902.
[33] Méndez I, Polšak A, Hudej R, Casar B. The Multigaussian method: a new approach to mitigating spatial heterogeneities with multichannel radiochromic film dosimetry. Phys Med Biol 2018;63:175013. https://doi.org/10.1088/1361-6560/aad9c1.
[34] Lewis D, Micke A, Yu X, Chan MF. An efficient protocol for radiochromic film dosimetry combining calibration and measurement in a single scan. Med Phys 2012;39:6339–50. https://doi.org/10.1118/1.4754797.
[35] Rivard MJ, Coursey BM, DeWerd LA, Hanson WF, Saiful Huq M, Ibbott GS, et al. Update of AAPM Task Group No. 43 report: a revised AAPM protocol for brachytherapy dose calculations. Med Phys 2004;31:633–74. https://doi.org/10.1118/1.1646040.
[36] Hiatt JR, Davis SD, Rivard MJ. A revised dosimetric characterization of the model S700 electronic brachytherapy source containing an anode-centering plastic insert and other components not included in the 2006 model. Med Phys 2015;42:2764–76. https://doi.org/10.1118/1.4919280.
[37] Devic S, Seuntjens J, Sham E, Podgorsak EB, Schmidtlein CR, Kirov AS, et al. Precise radiochromic film dosimetry using a flat-bed document scanner. Med Phys 2005;32:2245–53. https://doi.org/10.1118/1.1929253.
[38] Devic S, Tomic N, Soares CG, Podgorsak EB. Optimizing the dynamic range extension of a radiochromic film dosimetry system. Med Phys 2009;36:429–37. https://doi.org/10.1118/1.3049597.
[39] Ma C-M, Coffey CW, DeWerd LA, Liu C, Nath R, Seltzer SM, et al. AAPM protocol for 40–300 kV X-ray beam dosimetry in radiotherapy and radiobiology. Med Phys 2001;28:868–93. https://doi.org/10.1118/1.1374247.
[40] Taylor, Kuyatt C. Guidelines for evaluating and expressing uncertainty, for NIST measurement results NTN 1297. No Title n.d.
[41] McCabe BP, Speidel MA, Pike TL, Van Lysel MS. Calibration of GafChromic XR-RV3 radiochromic film for skin dose measurement using standardized X-ray spectra and a commercial flatbed scanner. Med Phys 2011;38:1919–30. https://doi.org/10.1118/1.3560422.
[42] Lewis D, Devic S. Correcting scan-to-scan response variability for a radiochromic film-based reference dosimetry system. Med Phys 2015;42:5692–701. https://doi.org/10.1118/1.4929563.
[43] Vera-Sánchez JA, Ruiz-Morales C, González-López A. Monte Carlo uncertainty analysis of dose estimates in radiochromic film dosimetry with single-channel and multichannel algorithms. Phys Medica 2018;47:23–33. https://doi.org/10.1016/j.ejmp.2018.02.006.
[44] Herskind C, Wenz F. Radiobiological aspects of intraoperative tumour-bed irradiation with low-energy X-rays (LEX-IORT). Transl Cancer Res 2014;3(1). February 2014 Transl Cancer Res (Intraoperative Radiother I).
[45] Massillon-JL G, Chiu-Tsao S-T, Domingo-Munoz I, Chan MF. Energy dependence of the new Gafchromic EBT3 film: dose response curves for 50 KV, 6 and 15 MV X-ray beams. Int J Med Phys Clin Eng Radiat Oncol 2012;01:60–5. https://doi.org/10.4236/ijmpcero.2012.12008.
[46] Sutherland JGH, Rogers DWO. Monte Carlo calculated absorbed-dose energy dependence of EBT and EBT2 film. Med Phys 2010;37:1110–6. https://doi.org/10.1118/1.3301574.
[47] Butson MJ, Cheung T, Yu PKN. Weak energy dependence of EBT gafchromic film dose response in the 50kVp–10MVp X-ray range. Appl Radiat Isot 2006;64:60–2. https://doi.org/https://doi.org/10.1016/j.apradiso.2005.07.002.
[48] Bekerat H, Devic S, DeBlois F, Singh K, Sarfehnia A, Seuntjens J, et al. Improving the energy response of external beam therapy (EBT) GafChromicTM dosimetry films at low energies (≤100 keV). Med Phys 2014;41:022101. https://doi.org/10.1118/1.4860157.
[49] Fogg P, Das KR, Kron T, Fox C, Chua B, Hagekyriakou J. Thermoluminescence dosimetry for skin dose assessment during intraoperative radiotherapy for early breast cancer. Australas Phys Eng Sci Med 2010;33:211–4. https://doi.org/10.1007/s13246-010-0019-3.
[50] Avanzo M, Dassie A, Chandra Acharya P, Chiovati P, Pirrone G, Avigo C, et al. Electron radiotherapy (IOERT) for applications outside of the breast: dosimetry and influence of tissue inhomogeneities. Phys Med 2020;69:82–9. https://doi.org/10.1016/j.ejmp.2019.12.003.
[51] Geleijns J, Wondergem J. X-ray imaging and the skin: radiation biology, patient dosimetry and observed effects. Radiat Prot Dosimetry 2005;114:121–5. https://doi.org/10.1093/rpd/nch544.
[52] White DR, Booz J, Griffith R V, Spokas JJ, Wilson IJ. Report 44. J Int Comm Radiat Units Meas 1989;os23:NP-NP. https://doi.org/10.1093/jicru/os23.1.Report44.
[53] Taylor REP. Monte Carlo Calculations for Brachytherapy. M. Sc. thesis. Carleton University, Ottawa, Canada, 2006.
[54] Zehtabian M, Faghihi R, Sina S. A review on main defects of TG-43, 2012. https://doi.org/10.5772/34360.
[55] Duque AS, Corradini S, Kamp F, Seidensticker M, Streitparth F, Kurz C, et al. The dosimetric impact of replacing the TG-43 algorithm by model based dose calculation for liver brachytherapy. Radiat Oncol 2020;15. https://doi.org/10.1186/s13014-020-01492-9.
[56] White SA, Landry G, Fonseca GP, Holt R, Rusch T, Beaulieu L, et al. Comparison of TG-43 and TG-186 in breast irradiation using a low energy electronic brachytherapy source. Med Phys 2014;41. https://doi.org/10.1118/1.4873319.